ChemElectroChem

Research Article
doi.org/10.1002/celc.202300374

Chemistry Europe
European Chemical Societies Publishing

www.chemelectrochem.org

Dynamic Electrochemical Impedance Spectroscopy for the Evaluation of Localised Corrosion on Aluminium Alloys

Erlind Mysliu,*[a] Thomas Holm,[b] Mattijs ten Cate,[c] and Andreas Erbe[a]

Dynamic electrochemical impedance spectroscopy (dEIS), an extension of conventional EIS, was used for rapid measurements of initiation of localised corrosion on 3005 aluminium alloys with different Mn (1.08–1.39 wt.%) and Cu (0.15–0.22 wt.%) content by evaluating the onset and evolution of a Faradaic process observed in 0.5 M Na_2SO_4 + 0.1 M NaCl. Differences between samples were detected with highest sensitivity from the charge transfer resistance during chronoamperometry at ca. 120 mV above the corrosion potential. These differences were caused by differences in pitting initiation, and correlated well with filament density from a filiform corrosion (FFC) test of samples coated with a 20 μm epoxy topcoat. The observation can be explained by the role of pitting in FFC initiation and the similarity in FFC propagation with pit growth. The results suggest that dEIS is an efficient method for screening alloys for their FFC susceptibility.

Introduction

Filiform corrosion (FFC) is a localised corrosion process typical for coated metals such as aluminium or magnesium.[1] The spread of threadlike filaments starting from coating defects is at the outset an aesthetic problem. However, FFC can in extreme cases lead to complete coating detachment, or trigger more severe types of corrosion such as pitting or intergranular corrosion. FFC usually starts at coating defects with a pit-like morphology ("successive pitting").[1,2] The pit-like environment at the coating defect develops into a filament by propagating horizontally at the interface between metal and coating, with actively corroding metal in the filament head. The propagation of the filament head, where the anodic metal dissolution takes place, leads to increased chloride concentration, and low pH, increasing the propensity for pitting. The aluminium alloys investigated here, from the 30XX series, are manufactured in sheets and are used, e.g., for household appliances and beverage cans. These alloys have excellent corrosion resistance but are quite sensitive to the presence of, e.g., Fe impurities. Such impurities reduce both corrosion performance and ductility of the alloy. The effect of Cu is controversial. In some cases there is an indication that Cu increases the susceptibility to FFC due to the formation of cathodic sites on the aluminium surface enhancing the corrosion process.[3] In other cases an increased amount of Cu does not result in an increased FFC susceptibility.[4] As far as Mn is concerned, both experiments and atomistic simulations show that Mn has a beneficial effect on the localised corrosion resistance of aluminium, either because of a reduced potential difference between matrix and intermetallic particles (IMPs) or the formation of a more compact surface oxide.[5,6]

The electrochemical properties of the surface have a major effect on FFC susceptibility. The correlation between FFC and the susceptibility to localised corrosion forms, such as pitting, has been already described multiple times.[7–10] The susceptibility to pitting corrosion of aluminium alloys has been characterised by several electrochemical techniques such as potentiodynamic polarisation,[11,12] chronoamperometry,[13] and electrochemical impedance spectroscopy (EIS).[14–16] The mechanism of pitting initiation and repassivation has been established based on the analysis of cyclic potentiodynamic polarisation curves.[12] As a result, the difference between pitting potential E_{pit} and repassivation potential E_{prot} emerged as an important parameter to assess the pitting susceptibility of different aluminium alloys. Chronoamperometry is one of the most appropriate techniques to evaluate and compare the pitting susceptibility.[13] EIS characterisation can produce results of accuracy that is not matched by other electrochemical or non-electrochemical techniques.[17] Thus, EIS has been widely used to investigate the surface properties of aluminium and to analyse its susceptibility to localised corrosion.[14,18–20] Local EIS, a specialised variant of scanning electrochemical microscopy,[21,22] has been used for studying coating performance,[23,24] and corrosion mechanisms.[25] A combination of different electrochemical techniques should thus yield information about localised corrosion in the system under investigation; it is anticipated that the sensitivity of a method combination must be higher than that of the individual methods.

During EIS the system under investigation needs to be linear and stable. A certain degree of non-linearity can be

[a] E. Mysliu, Prof. Dr. A. Erbe
Department of Materials Science and Engineering, NTNU, Norwegian, University of Science and Technology
7491 Trondheim, Norway
E-mail: erlind.mysliu@ntnu.no

[b] Dr. T. Holm
Institute for Energy Technology (IFE)
P.O. Box 40, 2027 Kjeller, Norway

[c] Dr. M. ten Cate
R&D Center Bonn, SPEIRA GmbH
Georg-von-Boeselager-Straße 21, 53117 Bonn, Germany

accepted if the higher harmonics generated are negligible with respect to the fundamental frequencies. For this reason a small signal amplitude is used during the excitation. The requirement of system stability limits the application of EIS to slowly changing systems.[26] However, neither the linearity nor the stability criteria are always strictly fulfilled in corroding systems especially when dealing with pitting initiation or repassivation. One method to study such processes is electrochemical noise analysis which, despite of recent progress in the time/frequency resolution,[27] has the limit that it relies on rather uncontrolled signal generation. Another relatively simple method may be the interleaved, fast measurement of a quantity such as the polarisation resistance,[28] which can however be difficult to interpret.

Dynamic Electrochemical Impedance Spectroscopy (dEIS) is a technique that enables the study of rapidly changing systems with EIS, and a combination of EIS with conventional electrochemical techniques such as chronoamperometry and potentiodynamic polarisation. Since its development in the 1990s,[29,30] the technique has evolved continuously. dEIS has been used, e.g., for the study of corrosion,[31,32] methanol oxidation,[33–35] fuel cells,[36,37] and electrocatalysis.[38] The technique is based on the application of a multisinusoidal perturbation instead of a sequential single sine. The advantage is that the total measurement duration t depends only on the duration of the experiment at the lowest frequency f included in the excitation signal, $t=\frac{n}{f}$, where n is the number of periods of the signal to be included in the measurement. Mostly prime numbered harmonics are chosen for excitation to avoid signal distortion from polyharmonics.[39,40]

The assumption that pitting and FFC are correlated stems from the similar environment and potential distribution that characterises an active pit and the head of a filament during the propagation step of FFC. However, the ratio between cathodic and anodic areas inside the head of the filament – although estimated to be of $\approx$100 – is very difficult to determine precisely. Electrochemical measurements in simulated environments have shown in certain cases a correlation between the corrosion current calculated from polarisation curves and the corrosion current calculated from FFC tests.[8,41] Although such correlation is not always straightforward,[9] it is qualitatively correct. Because of the difficulty of determining the correct area ratio between anodic and cathodic region and the Ohmic drop due to the electrolyte resistance any correlation between the electrochemical properties and corrosion properties shall be expected to be of qualitative nature. In other mechanisms of underpaint corrosion, correlation between corrosion current density and disbonding rate is also not always given.[42]

For this study, we use anodised 3005 aluminium alloys with Cu content in the range 0.15–0.22 wt.% and Mn content in the range 1.08–1.39 wt-%, i.e., with only relatively minor variations in composition. FFC tests were performed in order to assess the effect of Cu and Mn on the FFC performance of the different anodised samples. Starting with the hypothesis presented above that pitting susceptibility and FFC susceptibility in aluminium alloys are correlated, dEIS was used to investigate differences of electrochemical properties between the different alloy variants. Different methods of polarisation during dEIS were compared. Also, the repassivation behaviour was analysed by dEIS. The obtained ranking of the alloys was compared with results from FFC tests. Main goal of this work is to discriminate between very similar samples with slightly different FFC susceptibility by using dEIS under specific experimental conditions. Furthermore we evaluate the potential of dEIS in obtaining data concerning surface oxide breakdown and repassivation; such data are hardly obtainable by other, conventional electrochemical techniques.

Experimental methods

The investigated samples were EN AW-3005 T27 aluminium alloys (0.67 mm thickness) with a composition as shown in Table 1. Three samples have been electrochemically pretreated in sulphuric acid (with the label "An" in the table) to obtain a ca. 220 nm thick oxide layer.

All the electrochemical measurements were performed in a 0.5 M Na_2SO_4 + 0.1 M NaCl solution prepared using deionised water (18.2 MΩ cm^2, Millipore). The mildness of the electrolyte enables the extraction of small differences between the surface properties of the different samples.[10] The working electrode was the sample under investigation, a Pt foil was used as a counter electrode and the reference electrode was a Ag|AgCl (sat. KCl) electrode from Hach Lange Sensors. In this work, all electrode potentials are referred to Ag|AgCl (sat. KCl). In the first part of the experiment, the samples were left at open circuit potential (OCP) for 10 minutes. OCP was ca. −550 mV vs Ag|AgCl. Subsequently, samples were polarised in the anodic direction at three different potentials (−150 mV, −350 mV, −430 mV vs Ag|AgCl) always using a fresh specimen. The evolution of the dEIS spectra was recorded over time during polarisation. Each sample was kept at a certain potential until R_{ct} had fallen below 1 kΩ cm^2, indicating passivity breakdown. In the second part, after R_{ct} dropped below 1 kΩ cm^2, the potential was swept negatively at a sweep rate of 1 mV/s to observe the surface repassivation.

Dynamic impedance measurements were performed using a home developed set-up described in detail in Ref. [43] and schematically shown in Figure 1. A multisine signal generated by a Keithley KUSB-3116 was combined with a DC signal generated from a Model 175 Universal Programmer using an SRS SIM900 Mainframe with SIM910, SIM980, and SIM983 modules. The combined signal was sent to a Gamry reference 600 potentiostat and applied to the cell. The SIM900 Mainframe was also used to subtract the input DC signal from the measured potential. The measured current signal, the DC potential signal and the measured AC potential were

Table 1. Composition, in wt.%, of the four analysed EN AW-3005 samples. Samples with the designation "An" are anodised samples.

Elements	Cu_HMn_HAn	Cu_HMn_LAn	Cu_LMn_HAn	Cu_HMn_H
Si	0.50	0.49	0.48	0.50
Fe	0.59	0.58	0.55	0.59
Cu	0.22	0.22	0.15	0.22
Mn	1.39	1.08	1.39	1.39
Mg	0.34	0.35	0.35	0.34
Zn	0.22	0.14	0.08	0.22

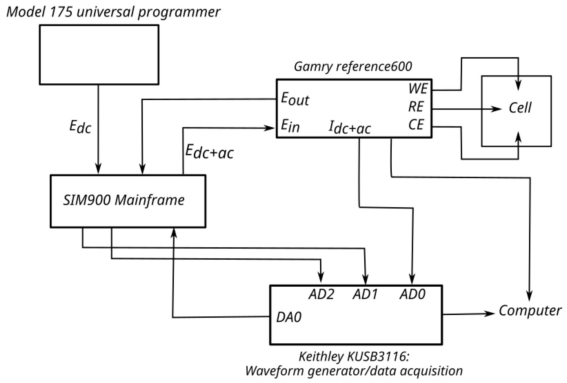

Figure 1. Schematic representation of the set-up used for dEIS measurements.

continuously sampled using the Keithley ADC/DAC module. Fast Fourier transform of the measured current and potential signal allowed the collection of the EIS spectra. The frequencies for the multisine signal generation are chosen following the method described by Popkirov and Schindler.[44] A phase randomisation of the excitation frequencies is used, and the amplitude of the individual sinewaves is halved for every decade of frequency increase. The total amplitude was scaled to a total maximum of 30 mV, and the frequency range was 13 kHz–1 Hz. The experimental data were fitted using the equivalent circuits shown in Figure 2. The collected dEIS data from this study is available online.[45]

The spectra representing the pit initiation and propagation were fitted using an equivalent circuit with one time constant, 1τ (Figure 2a). The spectra representing the repassivation were fitted using the equivalent circuit 2τ in Figure 2b. The data were if possible automatically fitted using the python impedance.py package.[46] A few more complex spectra were fitted using the ZSimpWin software using nonlinear least square fitting and the simplex algorithm. Two fitting approaches have been used because (i) impedance.py is fast and enables batch processing of large amounts of data, however, (ii) some spectra are more difficult to fit than others, such as in the case of a repassivating surface. For the latter, ZSimpWin becomes the most appropriate choice.

The anodised samples were industrially coil coated with an epoxy primer (5 μm dry film thickness) and an epoxy topcoat (20 μm dry film thickness). FFC tests were performed in an experienced industrial research lab according to DIN EN ISO 4623-2:2016, except for the initiation method. FFC was induced by dripping 37 wt.% HCl into the scribe such that the whole artificial defect was in contact with the solution. After 1 minute the solution was dabbed gently with laboratory paper. For evaluation of the tested samples, the average filament length $\bar{L}$, the filament density H, and the filiform number, $FN = H \times \bar{L}$, were determined. The filament length was determined by measuring the distance between the artificial scratch and the head of the filament. The average filament length was calculated by taking the average of the filament length of all

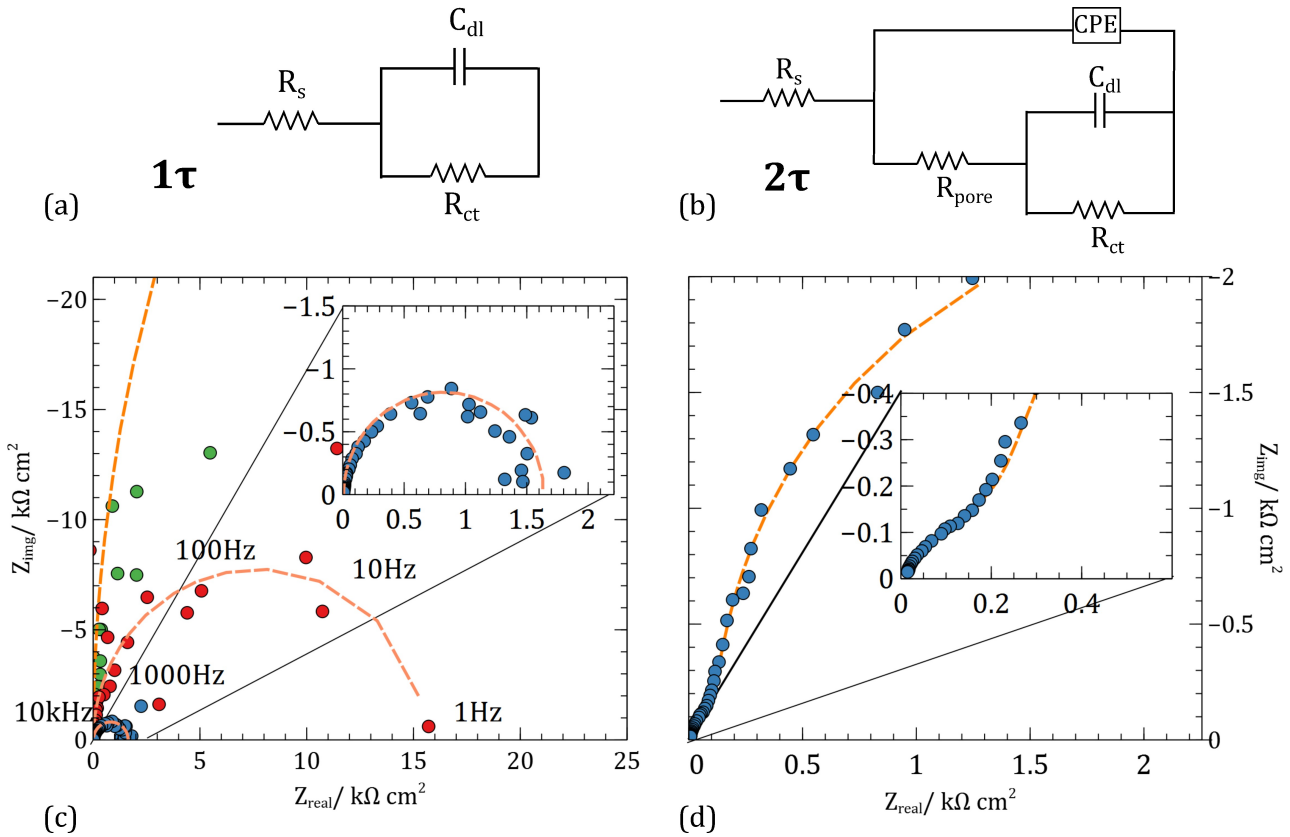

Figure 2. (a, b) Equivalent circuits used for fitting the data; R_s – solution resistance, R_{ct} – charge transfer resistance, C_{dl} – double layer capacitance, CPE – a constant phase element modelling the oxide film capacitance, R_{pore} – pore resistance in the oxide layer. (c, d) Examples of dEIS data from sample Cu_LMn_HAn, immersed in 0.1 M NaCl + 0.5 M Na_2SO_4 solution, fitted using the equivalent circuits showed in (a) and (b). In (c), the initiation and propagation of localised corrosion is shown as a combination of experimental data (circles) and fitting (dashed lines). The spectra where collected at different times when the sample was polarised at −430 mV. Panel (d) shows the surface impedance during repassivation at −655 mV, indicating the presence of 2 semicircles. The equivalent circuits shown in (a) and (b) will be referred to as 1τ and 2τ, respectively.

the filaments extending from the artificial scratch. The filament density was calculated by measuring the number of filaments extending from the artificial scratch and normalising it with respect to the length of the artificial scratch.

All the electrochemical measurements were performed on uncoated samples. Epoxy primer and epoxy topcoat were only applied for FFC testing.

Results

FFC test results are summarised in Table 2. Within the limited statistics of a typical corrosion study, there is no correlation between the amount of Cu present in the alloy and the FFC performance. On the other hand, an increase of Mn content in the alloy has a beneficial effect on FFC resistance. Anodised samples with an increased amount of Mn show a reduced filament density and filiform number.

Figure 2 shows an example of the EIS response obtained in this work, in this case the Cu_HMn_HAn sample. Panel c shows in a Nyquist plot the initiation of localised corrosion: The impedance spectrum evolved from an almost straight line (experimental points in green) to a semicircle (experimental points in blue). The straight line represents a "pure capacitance", sign of the presence of an intact aluminium oxide layer. When pitting corrosion is initiated, the formation of a semicircle in the Nyquist plot is reflecting the fact that a Faradaic current starts to contribute to the system's electrochemistry. In our case, the 1τ circuit shown in Figure 2a is used for this part of the analysis and an R_{ct} on the order of 100 kΩ is obtained. In panel d, a spectrum obtained during the repassivation (negative potential sweep) of one same sample is shown. Here, the presence of two semicircles is observed. The high frequency time constant is present probably because of the detection of the pore impedance. The detection of pore impedance could indicate the presence of damaged areas in the oxide caused by pitting corrosion.[47] The low frequency time constant is representative of the R_{ct} in parallel with the double layer capacitance C_{dl}.

R_{ct} can be estimated from the intersection of the fit curve with the Z_{real} axis. During the repassivation, the pore impedance R_{pore} can be extrapolated from the diameter of the semicircle at high frequency shown in the inset in Figure 2c.[48]

Figure 3 shows the evolution of the impedance spectra of the anodised samples with the best (Cu_HMn_HAn) and the worst (Cu_HMn_LAn) FFC resistance (c.f. FFC test results in Table 2) over time at three different potentials. The samples are polarised positively with respect to the open circuit potential and, due to the presence of chloride ions in solution, the breakdown of the oxide layer is expected. In the first part of the analysis, the spectrum is characteristic of a system that can be represented by a resistance (solution resistance) and a pure capacitance. As mentioned above, circuit 1τ is used for analysis of such spectra.

Comparing the two anodised samples with the best (Figure 3, upper spectra) and the worst (Figure 3, lower spectra) FFC resistance, the Nyquist plots show that the onset of the Faradaic process for the former is retarded with respect to the latter. Figure 4 shows the evolution of the R_{ct} for the three potentials. The differences from dEIS between the samples is largest when the potential is kept at −430 mV, i.e. closest to the OCP. The detected difference can be interpreted as showing the difference in pitting susceptibility between the samples.

Table 2. FFC test results for the anodised samples; average filament length $\bar{L}$, filament density H and the filiform number, $FN = H \times \bar{L}$.

Sample	H [1/cm]	$\bar{L}$ [mm]	FN [mm/cm]
Cu_HMn_HAn	0.4	1.1	0.04
Cu_HMn_LAn	1.5	1.2	0.18
Cu_LMn_HAn	0.8	1.3	0.12

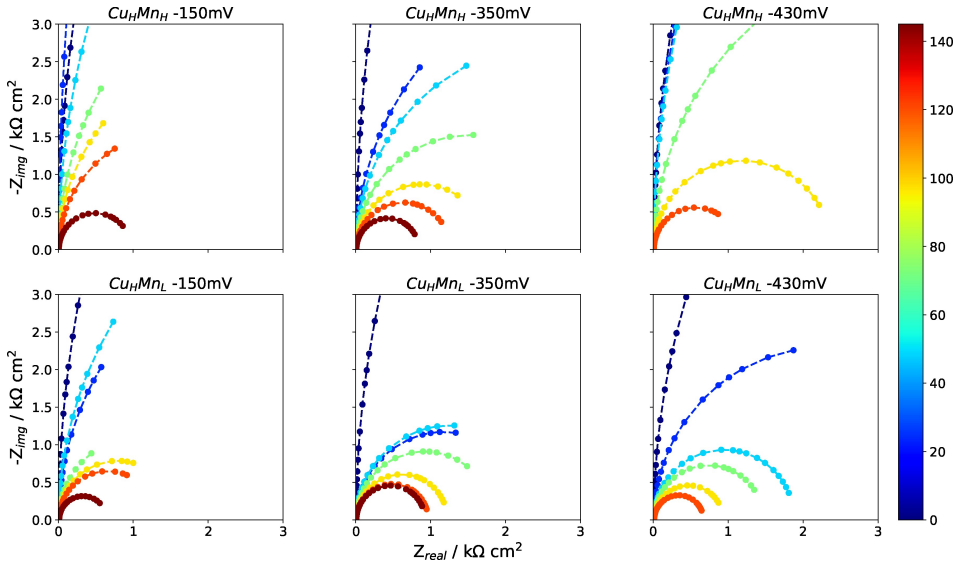

Figure 3. Evolution of Nyquist plot with time at constant potential. The potential at which the samples were held is written on the top of each plot. The colorbar indicates the time in minutes. For better visualisation of the trend, only the fit is shown.

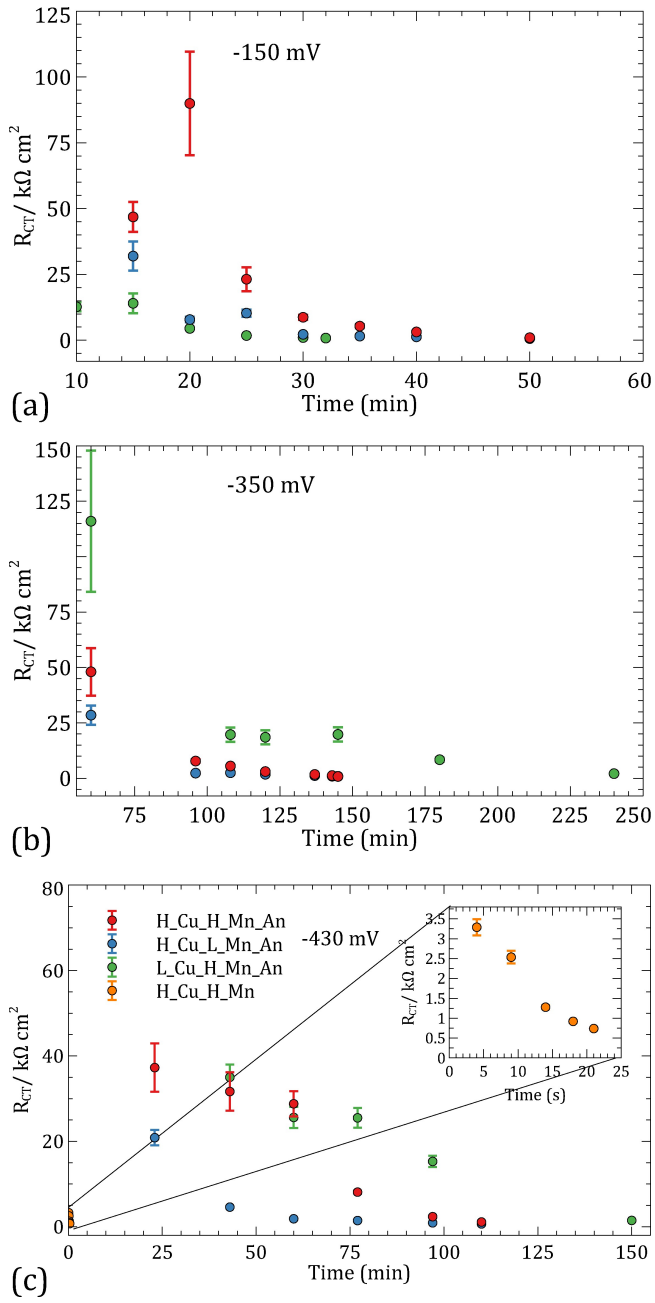

Figure 4. Charge transfer resistance R_{ct} evolution with time at three different potentials. −150 mV (a), −350 mV (b), and −430 mV (c). The inset in (c) shows the trend of the charge transfer resistance for the non-anodised sample which drops within the first seconds.

The time required until the onset of a Faradaic process becomes visible in the dEIS spectra can be considered an indication of the susceptibility towards localised corrosion of the sample. Furthermore, the diminishing of the R_{ct} with time indicates pit propagation. After a certain time, R_{ct} does not change anymore with time, probably because a limiting current has been reached. At this point the system must have reached a steady state of pit growth which also suppresses the initiation of new pits.[49]

The observed filiform frequency between the anodised samples ranges only from 0.4–1.5 filaments per cm (Table 2), i.e. there is a factor of ca. 3.5 between the sample with highest and lowest FFC susceptibility. When the difference in FFC resistance is that high, it is thus possible to discriminate between different samples based on their response recorded by dEIS. When testing a reference sample with much lower resistance to FFC (i.e., a non-anodised sample), the appearance of the semicircle in the Nyquist plot is observed after only a few seconds, demonstrating the high susceptibility towards a localised corrosion processes. For clarity, the change in R_{ct} with time of the non-anodised sample is only shown at −430 mV in Figure 4.

During the potential scan towards more negative potentials, surface repassivation is expected. In Figure 5, the radius of the semicircles in the Nyquist plots, indicating R_{ct}, increases while the potential is being swept towards more negative values, which is in line with the expectation of repassivation.

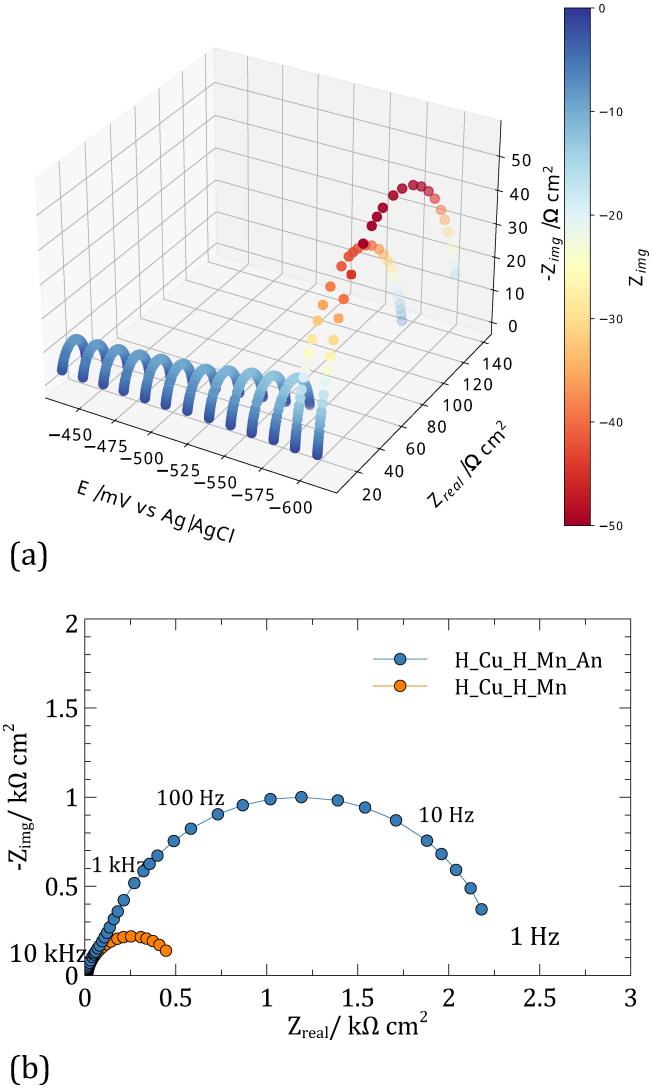

Figure 5. Evolution of Nyquist plot during the surface repassivation of Cu_HMn_HAn (a), and single impedance spectra taken during the repassivation of Cu_HMn_HAn (blue) and Cu_HMn_H (orange) at −625 mV to show the presence of two semicircles (b).

Furthermore, the spectra evolve into two semicircles, one at high and the other at low frequencies. The high frequency semicircle represents the impedance of pores in the oxide layer, presumably characterising the remains of the pits. The low frequency semicircle represents R_{ct} of Faradaic processes. The semicircle at low frequencies grows very rapidly when the potential becomes more negative, implying an increasing inhibition of electron transfer processes. The diameter of the semicircle at high frequency remains almost constant during the potential sweep, suggesting that the formation of new pores is not taking place during this step.

Discussion

There is the expected anti-correlation between filament density H and R_{ct}, i.e. $H \sim \frac{1}{R_{ct}}$ (Figure 6). It must be stressed that the amount of samples measured here is low. Notwithstanding this comparatively poor statistics, the differences on both the R_{ct} scale and the H scale are very similar when normalised to the total difference. In other words, the difference in R_{ct} between Cu_HMn_HAn and Cu_LMn_HAn is smaller than the difference between the latter and Cu_HMn_LAn, while the same is valid for the filament density. Consequently, results presented in Figures 3 and 4 demonstrate that dEIS can be used to assess the localised corrosion resistance of aluminium alloys. The corrosion resistance is quantified through the measurement of R_{ct}, where a high value is desirable.

Most of the samples studied here are anodised samples, and clearly, if a non-anodised sample of the same composition is used (Figure 4c), R_{ct} decay starts almost immediately, indicating faster onset of localised corrosion. Therefore, the method proposed is most suitable for the study of anodised samples designed to have low localised corrosion rates. The method can, however, be adapted via the polarisation potential, the polarisation time, and if needed the electrolyte.

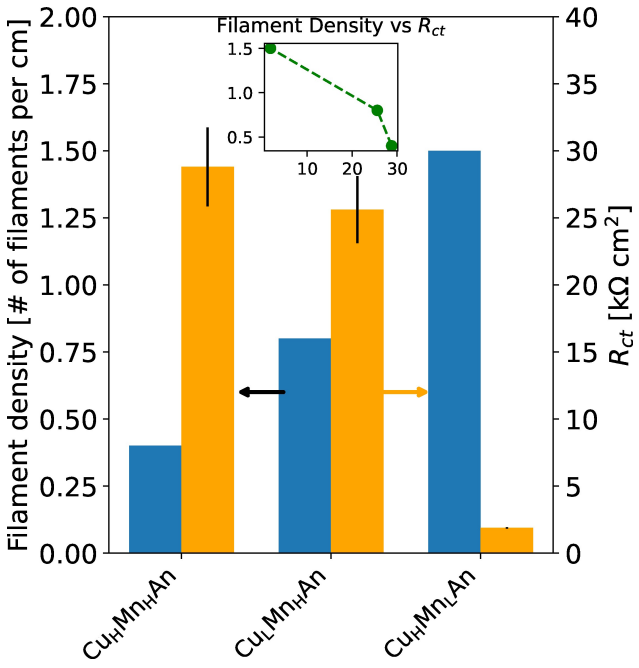

Figure 6. Correlation between R_{ct} from the measurement at −430 mV after 1 hour of exposure, and filament density H for the three anodised samples.

For discrimination of localised corrosion properties between different samples, as in this case anodised aluminium, a method is desired which (i) can clearly distinguish samples, (ii) is as fast as possible, and (iii) easy to use. When comparing the different potentials in Figure 4, it is evident that the lower potentials, −350 mV and −430 mV, are better suited to distinguish between the samples. Ranking for pitting susceptibility obtained from these holding potentials is also internally consistent, as both suggest the order $Cu_LMn_HAn \geq Cu_HMn_HAn > Cu_HMn_LAn$. The largest separation between samples is observed for the holding potential of −430 mV. A polarisation time in the range 35–75 min is most suitable, as there is a clear difference between the samples. Thus, the proposed method to rank materials in terms of pitting and FFC susceptibility by dEIS in 0.5 M Na_2SO_4 + 0.1 M NaCl is:

1. Hold the samples at the open-circuit potential for 10 minutes
2. Polarise the sample to −430 mV vs Ag|AgCl and measure dEIS at a 1 s resolution
3. Fit the EIS spectra obtained after 40 minutes using the R(CR) circuit (1τ), or a more appropriate circuit
4. Extract and normalise the R_{ct} parameter with respect to sample area. A value below 20 kΩ cm^2 indicates that localised corrosion has been initiated and that the sample is susceptible to localised corrosion, including FFC.

The method suggested here still needs validation and further testing. Nevertheless, the dEIS method shows potential for providing a quantification of localised corrosion properties in less than 1 h of testing with minimal sample preparation compared to accelerated corrosion tests such as FFC testing. Based on the general electrochemical properties of aluminium, we expect, however, that both the potential window and the time window indicated here is applicable to a series of alloys. This expectation builds on the similarities of the corrosion potential of many alloys in chloride containing medium, and consequently similarities for difference between corrosion potential and polarisation potential.

In case of dEIS, the charge transfer resistance which can be extracted by fitting the spectra, is a differential resistance at a certain potential and is given by:

$$\left(\frac{dE}{dI}\right)_E = R_{ct}$$

The difficulty in determining the composition of the solution and the area ratio between anodic and cathodic sites inside a filament during FFC and the differential nature of the R_{ct} makes it difficult to have a quantitative correlation between results obtained from electrochemical measurements and FFC tests. Furthermore, obtaining significant quantitative results is challenging when both the amount of samples used for FFC testing and the number of samples with different composition are limited.

The main difference between the samples used in this work is the ratio of Cu and Mn in the samples. The susceptibility to localised corrosion is related to the presence of IMPs,[50] the different distribution of elements such as Mn between solid solution and IMPs,[5,51] and inhomogeneities of the oxide layer or the oxide layer thickness.[52] The structure and composition of the metallic surface or surface oxide layer determines its electrochemical features and reactivity towards electron and ion transfer. Previous studies have shown that the presence of alloying elements included in the surface oxides leads to the modification of the oxide electronic structure.[53–56] For aluminium, a linear correlation between pitting and flat band potential has been reported.[53] However, this aspect won't be further discussed here. The sensitivity of dEIS towards the global interface electrochemical features allows for the discrimination between surfaces with different susceptibility towards localised corrosion, despite the relatively similar composition of the alloy. A full description of the metallurgical reasons for the differences required detailed microstructural analysis and is beyond the scope of this work.

Some spectra recorded show an inductive behaviour at low frequency and at certain potentials. The inductive behaviour has been associated with metal dissolution without oxide formation related to the negative differential effect[57] but also with the adsorption of reaction intermediates in the case of Mg,[58] or Al corrosion.[59] A candidate intermediate for this system here could be a hydride species.[2,28,60] The evolution of the inductive loop with time or potential could be used for the study of the reaction mechanism that can in turn be related to different surface pretreatments or electrolyte conditions. Figure 5 demonstrates the possibility of following the evolution of parameters such as R_{ct}, C_{dl}, R_{pore} and the CPE as a function of time and thus potential for the different samples. The relation between these different elements and the current density can give an insight into the movement of ions through, for example, the oxide layer, and therefore help explain the mechanism of repassivation.[32,61] In general, dEIS has a depth of information that is higher than conventional electrochemical techniques such as potentiodynamic polarisation, and it can be used in addition or as a supplement to specialised techniques developed for local corrosion studies such as local electrochemical impedance spectroscopy.[21,22]

Conclusions

In this work dEIS was used to study localised corrosion on different EN AW-3005 surfaces.

1. dEIS is suitable for studying passivity breakdown and repassivation. Passivity breakdown is an important prerequisite of localised corrosion on aluminium alloys. The time resolution of dEIS enables the extraction of a wealth of information on breakdown and reformation of oxide layers.
2. Passivity breakdown as sensed via dEIS correlated well with FFC resistance for anodised EN AW-3005 after an appropriately selected polarisation protocol. Thus, dEIS can be used to compare the FFC resistance of aluminium alloys in a much shorter experiment than conventional corrosion tests. This correlation can be explained by the fact that pitting which is caused by passivity breakdown initiates FFC. Nevertheless, with the current protocol, a qualitative screening of aluminium samples can be done.
3. For the alloys investigated here, Mn has a beneficial effect on the FFC performance while there is no observed correlation between the Cu concentration and the FFC resistance.

Author Contributions

Erlind Mysliu: Conceptualization; Formal analysis (dEIS); Investigation (dEIS); Methodology; Visualization; Writing – original draft; Writing – review & editing.

Thomas Holm: Methodology, Writing – original draft, Writing – review & editing.

Mattijs ten Cate: Formal analysis (FFC test); Funding acquisition; Investigation (FFC test); Project administration; Resources; Writing – review & editing.

Andreas Erbe: Conceptualization; Funding acquisition; Project administration; Supervision; Writing – review & editing.

Acknowledgements

This work was part of the project "Coated Recycled Aluminium – developing surfaces for well-adhering and corrosion resistant coating systems" supported by the Research Council of Norway (No. 309875), Hydro and Speira. The authors acknowledge Frode Seland and Magdalena Müller for useful discussions and for helping with the equipment set-up.

Conflict of Interests

There are no conflicts of interest to declare.

Data Availability Statement

The raw data associated to this study will be made available via NTNU's institutional repository https://doi.org/10.18710/Z6P6SE.

Keywords: Alloys · Anodised Aluminium · Dynamic Electrochemical Impedance Spectroscopy · Electrochemistry · Localised Corrosion · Pitting Corrosion

[1] H. N. McMurray, G. Williams, *Shreir's Corrosion*, chapter 2.14 – Under Film/Coating Corrosion, pages 988–1004, Elsevier, Oxford **2010**.
[2] E. Mysliu, O. Lunder, A. Erbe, *Phys. Chem. Chem. Phys.* **2023**, *25*, 11845.
[3] A. Afseth, J. Nordlien, G. Scamans, K. Nisancioglu, *Corros. Sci.* **2002**, *44*, 2543.
[4] P. Premendra, H. Terryn, J. M. C. Mol, J. H. W. de Wit, L. Katgerman, *Mater. Corros.* **2009**, *60*, 399.
[5] M. Zamin, *Corrosion* **1981**, *37*, 627.

[6] J. Chen, J. Xiao, J. Poplawsky, F. M. Michel, C. Deng, W. Cai, *Corros. Sci.* **2020**, *173*, 108749.
[7] V. Poulain, J.-P. Petitjean, E. Dumont, B. Dugnoille, *Electrochim. Acta* **1996**, *41*, 1223.
[8] J. Mol, B. R. W. Hinton, D. van der Weijde, J. de Wit, S. van der Zwaag, *J. Mater. Sci.* **2000**, *35*, 1629.
[9] J. Mol, J. van de Langkruis, J. de Wit, S. van der Zwaag, *Corros. Sci.* **2005**, *47*, 2711.
[10] M. Fedel, C. Zanella, L. Ferrari, F. Deflorian, *Electrochim. Acta* **2021**, *381*, 138288.
[11] B. Zaid, D. Saidi, A. Benzaid, S. Hadji, *Corros. Sci.* **2008**, *50*, 1841.
[12] M. Trueba, S. P. Trasatti, *Mater. Chem. Phys.* **2010**, *121*, 523.
[13] T. Vignoli Machado, P. Atz Dick, G. H. Knörnschild, L. F. Dick, *Surf. Coat. Technol.* **2020**, *383*, 125283.
[14] Y. Huang, H. Shih, H. Huang, J. Daugherty, S. Wu, S. Ramanathan, C. Chang, F. Mansfeld, *Corros. Sci.* **2008**, *50*, 3569.
[15] J. F. Li, Z. Q. Jia, C. X. Li, N. Birbilis, C. Cai, *Mater. Corros.* **2009**, *60*, 407.
[16] L. L. Wei, Q. L. Pan, L. Feng, Y. L. Wang, H. F. Huang, *Mater. Corros.* **2015**, *66*, 54.
[17] F. Mansfeld, M. W. Kendig, *J. Electrochem. Soc.* **1988**, *135*, 828.
[18] G. S. Peng, K. H. Chen, H. C. Fang, H. Chao, S. Y. Chen, *Mater. Corros.* **2010**, *61*, 783.
[19] P. Carbonini, T. Monetta, D. B. Mittoni, F. Bellucci, P. Mastronardi, B. Scatteia, *J. Appl. Electrochem.* **1997**, *27*, 1135.
[20] B. Usman, M. Curioni, *Corros. Sci.* **2021**, *192*, 109772.
[21] O. Gharbi, K. Ngo, M. Turmine, V. Vivier, *Curr. Opin. Electrochem.* **2020**, *20*, 1.
[22] V. M. Huang, S.-L. Wu, M. E. Orazem, N. Pébère, B. Tribollet, V. Vivier, *Electrochim. Acta* **2011**, *56*, 8048.
[23] R. S. Lillard, J. Kruger, W. S. Tait, P. J. Moran, *Corrosion* **1995**, *51*, 251.
[24] L. V. S. Philippe, G. W. Walter, S. B. Lyon, *J. Electrochem. Soc.* **2003**, *150*, B111.
[25] G. Baril, C. Blanc, M. Keddam, N. Pebere, J . *Electrochem. Soc. Interface* **2003**, *150*, B488.
[26] A. Lasia, Conditions for Obtaining Good Impedances, Electrochemical Impedance Spectroscopy and its Applications, pages 271–300, Springer, New York, NY **2014**.
[27] I. Jevremovic, A. Erbe, *Phys. Chem. Chem. Phys.* **2019**, *21*, 24361.
[28] E. Mysliu, K. S. Storli, E. Kjørsvik, O. Lunder, A. Erbe, *J. Electrochem. Soc.* **2023**, *170*, 011503.
[29] D. A. Harrington, *J. Electroanal. Chem.* **1993**, *355*, 21.
[30] M. E. van der Geest, N. J. Dangerfield, D. A. Harrington, *J. Electroanal. Chem.* **1997**, *420*, 89.
[31] K. Darowicki, S. Krakowiak, P. Slepski, *Electrochim. Acta* **2004**, *49*, 2909.
[32] K. Darowicki, S. Krakowiak, P. Slepski, *Anti-Corros. Methods Mater.* **2010**, *57*, 2909.
[33] P. K. Dahlstrom, D. A. Harrington, F. Seland, *ECS Trans.* **2012**, *41*, 35.
[34] T. Holm, P. K. Dahlstrøm, S. Sunde, F. Seland, D. A. Harrington, *Electrochim. Acta* **2019**, *295*, 139.
[35] T. Holm, S. Sunde, F. Seland, D. A. Harrington, *Electrochim. Acta* **2019**, *323*, 134764.
[36] M. Darab, P. K. Dahlstrøm, M. S. Thomassen, F. Seland, S. Sunde, *J. Power Sources* **2013**, *242*, 447.
[37] K. Darowicki, E. Janicka, M. Mielniczek, A. Zielinski, L. Gawel, J. Mitzel, J. Hunger, *Electrochim. Acta* **2018**, *292*, 383.
[38] R. L. Sacci, F. Seland, D. A. Harrington, *Electrochim. Acta* **2014**, *131*, 13.
[39] G. Popkirov, R. Schindler, *Electrochim. Acta* **1995**, *40*, 2511.
[40] G. Popkirov, *Electrochim. Acta* **1996**, *41*, 1023.
[41] A. Cristoforetti, S. Rossi, F. Deflorian, M. Fedel, *Prog. Org. Coat.* **2023**, *179*, 107525.
[42] D. Iqbal, J. Rechmann, A. Bashir, A. Sarfraz, A. Altin, A. Erbe, *Mater. Corros.* **2019**, *70*, 481.
[43] R. L. Sacci, D. Harrington, *ECS Trans.* **2009**, *19*, 31.
[44] G. S. Popkirov, R. N. Schindler, *Rev. Sci. Instrum.* **1993**, *64*, 3111.
[45] E. Mysliu, T. Holm, A. Erbe, Replication data for: "Dynamic Electrochemical Impedance Spectroscopy for the Evaluation of Localised Corrosion on Aluminium Alloys", NTNU Open Research Data, https://doi.org/10.18710/Z6P6SE **2023**.
[46] M. D. Murbach, B. Gerwe, N. Dawson-Elli, L. kun Tsui, *J. Open Source Softw.* **2020**, *5*, 2349.
[47] T. Sharma, T. Holm, J. Diaz-Real, W. Mérida, *Electrochim. Acta* **2019**, *317*, 528.
[48] N. Celati, M. Sainte Catherine, M. Keddam, H. Takenouti, *Mater. Sci. Forum* **1995**, *192*, 335.
[49] T. Li, J. R. Scully, G. S. Frankel, *J. Electrochem. Soc.* **2018**, *165*, C762.
[50] A. Afseth, J. Nordlien, G. Scamans, K. Nisancioglu, *Corros. Sci.* **2001**, *43*, 2093.
[51] H. Mraied, W. Cai, A. A. Sagüés, *Thin Solid Films* **2016**, *615*, 391.
[52] M. B. Spoelstra, A. J. Bosch, D. H. van der Weijde, J. H. W. de Wit, *Mater. Corros.* **2000**, *51*, 155.
[53] E. McCafferty, *Corros. Sci.* **2003**, *45*, 301.
[54] G. Tranchida, M. Clesi, F. Di Franco, F. Di Quarto, M. Santamaria, *Electrochim. Acta* **2018**, *273*, 412.
[55] E. McCafferty, *J. Electrochem. Soc.* **1999**, *146*, 2863.
[56] P. M. Natishan, E. McCafferty, G. K. Hubler, *J. Electrochem. Soc.* **1988**, *135*, 321.
[57] M. Curioni, L. Salamone, F. Scenini, M. Santamaria, M. Di Natale, *Electrochim. Acta* **2018**, *274*, 343.
[58] G. Baril, G. Galicia, C. Deslouis, N. Pébère, B. Tribollet, V. Vivier, *J. Electrochem. Soc.* **2006**, *154*, C108.
[59] L. Péter, J. Arai, H. Akahoshi, *J. Electroanal. Chem.* **2000**, *482*, 125.
[60] S. Adhikari, J. Lee, K. R. Hebert, *J. Electrochem. Soc.* **2008**, *155*, C16.
[61] K. Darowicki, S. Krakowiak, P. Slepski, *Electrochem. Commun.* **2004**, *6*, 860.

Manuscript received: July 31, 2023
Revised manuscript received: September 11, 2023
Version of record online: October 24, 2023